

Buckling Behavior and Structural Efficiency of Open-Section Stiffened Composite Compression Panels

Jerry G. Williams* and Manuel Stein†
NASA Langley Research Center, Hampton, Va.

Several exploratory experiments with *J*- and blade-stiffened graphite/epoxy panels were conducted to obtain insight into how well experimental data could be correlated with analysis for the buckling behavior of open-section stiffened composite compression panels. Although some nonlinear behavior was observed during the experiments, adequate correlation with analysis was obtained to justify the use of linear, thin-plate buckling analysis in a minimum-weight design synthesis program for *J*- and blade configurations. Results from two design studies using this program are presented. In the first study the minimum weights of *J*- and blade-configurations for two different material systems (graphite/epoxy and aluminum) are determined subject to buckling and strength constraints for a wide range of the compressive load index. In the second study the minimum weights required for graphite/epoxy blade-stiffened panels to satisfy additional stiffness constraints typical of medium-size commercial aircraft wing structures are determined. Both minimum-weight studies indicate that graphite/epoxy open-section stiffened panels can be designed so that weight savings of 30% to 50% are possible compared with the most efficient aluminum designs.

Nomenclature

A	= area
B	= panel width
B_i	= dimension of panel segment i
E_{11}	= lamina modulus in fiber direction
E_{22}	= lamina modulus transverse to fiber direction
G_{12}	= lamina shear modulus
K	= structural efficiency coefficient
L	= panel length
\bar{N}	= buckling stress resultant
P_e	= Euler buckling load
T_i	= thickness of layer in segment i
W	= panel weight
ϵ	= strain
ν_{12}	= major Poisson's ratio
ρ	= density
\bar{N}/L	= load index
W/AL	= weight index

Introduction

USE of advanced filamentary composites in aircraft structures has the potential for decreasing structural weight. Weight savings are made possible because of the high stiffness-to-density and high strength-to-density ratios of filaments such as those made of graphite and boron. Also, weight may be saved by tailoring the ply thicknesses and orientations of layered composites to meet specific structural needs. New fabrication techniques made possible by composites may also result in fewer parts and could reduce the assembly time and costs of aircraft structures. To take advantage of the potential weight savings offered by composites, it is necessary to establish design methods for a variety of structural configurations. One composite configuration which has been studied in detail is the hat-stiffened panel. Analytical and experimental investigations of hat-stiffened graphite/epoxy panels have shown that this configuration can carry a

specified compression load with less weight than is required for most other configurations.^{1,2} A study of compression panels for commercial aircraft wings³ indicates that open-section stiffened composite panels such as *J*- and blade-stiffened configurations offer attractive design alternatives when compared with closed-section stiffened panels such as the hat configuration. The present study is concerned with design and analysis procedures necessary to determine the minimum-weight of open-section stiffened panels required to carry a specified axial compression load.

Buckling is a constraint which must be satisfied in the design of minimum-weight compression panels. Simple closed-form local buckling and column buckling formulas have been found to be adequate for the design of closed-section configurations such as the hat.² More exact buckling analyses, however, are required to predict accurately the buckling behavior of open-section configurations due to their more complicated stiffener twisting behavior. Twisting effects include overall stiffener torsion coupled with local bending of the stiffener web. These buckling modes are interdependent and considerable interaction between stiffener twisting effects and local and column buckling modes can occur. In the past, stiffener twisting mode buckling was avoided in open-section metal panels by applying simple criteria based on experience to determine the appropriate relative proportions of the panel segments. Such criteria have not yet been obtained for open-section stiffened composite panels and dependence must be placed on proven analytical procedures to describe this complicated buckling behavior. Sophisticated computer codes are available which provide the exact solution for the buckling of open-section stiffened panels that include stiffener twisting effects. These solutions are exact in that they satisfy all the conditions of the problem within the limits of linear elastic, Kirchhoff thin-plate theory. In this paper, use is made of three such codes, STAGS,⁴ BUCCLASP-2,⁵ and VIPASA.⁶ The STAGS code is based on a two-dimensional finite-difference technique and will satisfy any imposed boundary conditions; BUCCLASP-2 and VIPASA link together an assembly of plate segment solutions for panels with simply-supported ends.

Even "exact" analytical solutions have limitations which may be important in comparing theory with experiment. Linear elastic thin-plate theory does not address initial imperfection effects, and the effect of transverse shear deformations through the thickness of the plate segments is not included. Initial imperfection effects can be studied using the

Presented at the AIAA/ASME/SAE 17th Structures, Structural Dynamics, and Materials Conference, Valley Forge, Pa., May 5-7, 1976; submitted May 10, 1976; revision received August 6, 1976.

Index categories: Aircraft Structural Design (Including Loads); Structural Composite Materials (Including Coatings); Structural Design, Optimal.

*Aerospace Engineer. Member AIAA.

†Aerospace Engineer. Associate Fellow AIAA.

nonlinear option of the STAGS code. (The buckling studies based on STAGS presented in this paper make use of the linear bifurcation option.) To obtain initial insight into the agreement to be expected between experiment and analysis for the buckling behavior of open-section configuration composite panels, several exploratory experiments were conducted. For the panels considered in this study, the experimental and analytical comparison showed sufficiently adequate correlation to justify using thin-plate buckling analysis procedures in the next phase of the study: the development of a minimum-weight design synthesis code for open-section stiffened panels.

A design synthesis code called JPOP (*J* Panel Optimization Procedure) has been developed for the design of minimum-weight open-section stiffened panels loaded in axial compression with either *J*- or blade-configuration geometry. The dimensions and thicknesses of the configuration cross section are the design variables and the constraints are buckling and strength. The analysis used to formulate the buckling constraint is a simplified analysis developed especially for this purpose (described in Appendix A). The simplified buckling analysis is sufficiently refined to include all of the important buckling modes characteristic of open-section stiffened panels including stiffener twisting behavior and requires considerably less computational time than the exact solution codes discussed earlier. A comparison of the buckling strains obtained from the simplified and exact analyses for typical *J*- and blade-configuration designs is presented in Appendix B. Minimum weight *J*- and blade-panel results obtained using the JPOP procedure are presented in the form of a structural efficiency chart for easy comparison.

A potential application of composites for wing structures of commercial aircraft could be the replacement (retrofit) of the wing boxes of existing aircraft with a graphite/epoxy structure. For such an application, it is desirable, for considerations such as aeroelastic behavior, fatigue limits and load transfer, to match closely the bending and torsional stiffness of the existing wing structure. In Ref. 3, the bending and torsional stiffnesses of a wing have been converted into extensional and shear stiffnesses of typical wing panels. When sufficient material is added to provide additional stiffnesses to match those of commercial aircraft, it can be shown³ that all the usual graphite-epoxy configurations meet these requirements with approximately the same weight. The geometric simplicity of the blade configuration makes it an attractive structural candidate, and it was chosen for a minimum-weight design study in which extensional and shear stiffness constraints associated with retrofit wing designs were imposed in addition to the buckling and strength constraints. Results of this study are also presented on a structural efficiency graph, and the potential weight savings compared to present aluminum wing designs are indicated.

Buckling of Open-Section Stiffened Compression Panels

Characteristic Buckling Modes

Calculations for structural efficiency require determination of the loads (or strains) at which structures buckle in various possible modes. The modes of buckling of open-section stiffened panels can be classified as local, twisting, and column buckling. Interactive modes between these three general classes are also characteristic of open-section stiffened panels such as those shown for the *J*-configuration in Fig. 1. Shown are two local modes—one where the skin alone (denoted by local/skin hereafter) is deformed and one involving deformations of the skin and web; two twisting modes—one involving deformations of the skin and web and one where the web bends (or rolls) independent of the skin; and two column modes—one where the web bends (or rolls) in combination with column translation and one where it does not. These buckling modes are obtained from exact analysis solutions.

Local modes are usually associated with short buckle wavelength on the order of the width of the individual plate segments. Column modes are observed at long wavelength, and twisting modes occur for wavelengths, that are between the wavelength associated with local and column buckling. A physical interpretation for coupled modes can be obtained by considering that skin buckling forces the web to roll for the local/skin and web mode, and that the web forces the skin to deform for the twisting/skin and web mode. For sufficiently long panels, the web does not roll and buckling is a column buckling mode. Similar mode shapes are observed for the blade configuration, but the local/skin and web modes do not occur due to the absence of the outstanding flange.

Experimental Studies and Analytical Comparisons

Specimen Description and Test Technique

Graphite/epoxy open-section stiffened panels of *J*- and blade-configurations were selected for experimental evaluation and comparison with exact analysis buckling results. Specimens were constructed using unidirectional filamentary graphite/epoxy tape and the integral assemble was vacuum bagged and autoclave cured. Photographs and dimensions of the specimens are presented in Fig. 2. The *J*-configuration chosen for test has minimum weight panel proportions that satisfy buckling and strength constraints ($W/AL = 5.70 \text{ kg/m}^3 (2.06 \times 10^{-4} \text{ lb/in.}^3)$ and $N/L = 0.689 \text{ MPa (100 lb/in.}^2)$). The blade-configuration chosen was also a minimum-weight design, but had additional stiffness requirements typical of medium-size commercial aircraft wing structures ($W/AL = 11.3 \text{ kg/m}^3 (4.10 \times 10^{-4} \text{ lb/in.}^3)$ and $N/L = 2.07 \text{ MPa (300 lb/in.}^2)$). The *J*-stiffened panel with two stiffeners was tested with panel lengths of 27.7, 40.6, and 76 cm. The axial stiffness of the *J*-stiffened panels was 22.5 MN (5.06 Mlbf). A 76-cm long *J*-stiffened panel simply supported on the loaded ends was designed to be critical in buckling at an axial strain of 0.003. The blade-stiffened specimens with three stiffeners were tested with panel lengths of 18.3, 27.7, 30.7, and 76 cm. The axial stiffness of the blade-stiffened panels was designed to buckle at an axial strain of 0.0036 for a 76-cm-long simply supported specimen. As shown in Fig. 2, the ends of the specimens were potted in an epoxy compound (approximately 2.5 cm thick) to facilitate flat-end testing. Flat-end testing of a panel with potted ends results in essentially clamped boundary conditions. The lateral edges of the specimens were unsupported. The experimental buckling strains were obtained from strain reversal data. During testing moiré fringe patterns⁷ of the buckle mode were photographed. These fringe patterns can be thought of as a contour map of the lateral deflections of the panel surface. Displacements of the crosshead platens and of selected points on the specimen cross section were recorded during the tests.

Analytical Models

Experimental results for the two configurations were compared with two sets of analytical results, one for the loaded end boundary conditions clamped (calculated using the STAGS computer code) and the other for simple support boundary conditions (calculated using the BUCASP-2 computer code). The lateral edges for both theoretical solutions are free. Prior to buckling, the loaded edges for the clamped solutions are restrained from inplane motion ($v=0$), whereas for the simple support solutions they are free to expand ($\tau_{xy}=0$). The clamped solution, therefore, accounts for the biaxial prebuckling stress field that develops in the experiment due to the Poisson effect. Although the simple support solutions do not model the test conditions, they were included for comparison since they help provide insight into open-section panel buckling behavior. Analytical models are based on the nominal dimensions given in Fig. 2 and material properties listed in Table 1.

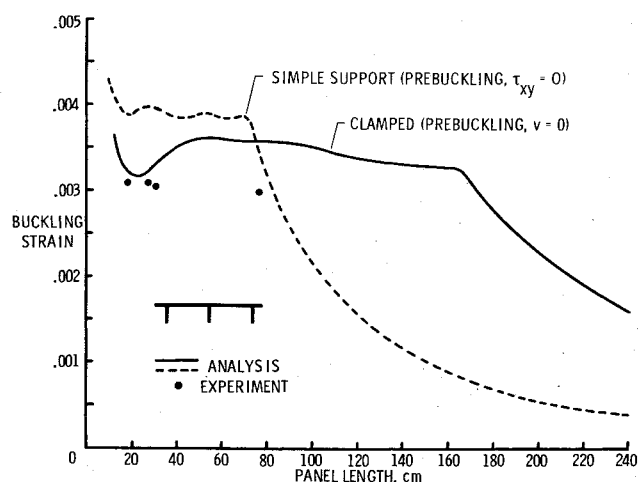


Fig. 5 Critical buckling strain as a function of panel length for graphite/epoxy blade-stiffened panel. (Specimen ends potted and flat-end tested).

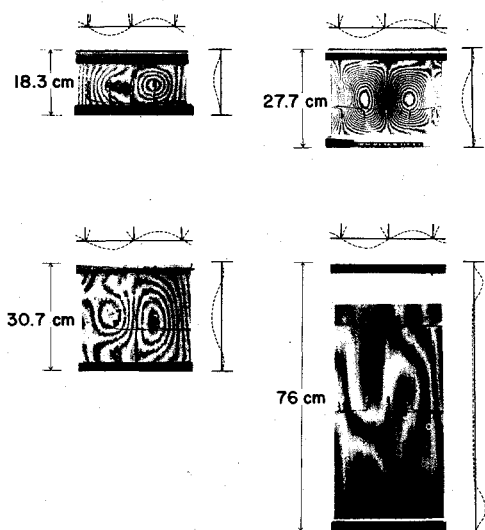


Fig. 6 Experimental and analytical comparison of mode shapes for graphite/epoxy blade stiffened panels.

Blade-Stiffened Specimens

Experimental buckling strains for the four blade-stiffened specimens are presented in Fig. 5 and compared with the theoretical buckling strains for clamped and simple support boundary conditions. For panel lengths less than 70 cm, the biaxial stress field near the ends causes the clamped solution to have lower buckling strains than the laterally unrestrained simple support solution. Poisson's ratio ν_{12} for the skin laminate, which has one-third 0° oriented material and two-thirds $\pm 45^\circ$ oriented material, is 0.675 compared with 0.718 for an all $\pm 45^\circ$ laminate. Experimental results are in excellent agreement with the clamped solution for the three shorter length specimens. The buckling strain for the 76-cm-long specimen is 16% below the clamped end linear elastic thin-plate solution. For panel lengths greater than 170 cm, the Euler column buckling strain is critical, the lateral end restraint is no longer a dominant factor, and the clamped solution is approximately four times the simple support solution.

The moiré fringe patterns shown in Fig. 6 all represent the skin side of the blade-stiffened specimens. The mode shape for the 76-cm-long specimen indicates that the biaxial stress field causes localized buckling in the end regions. These effects spread out into the center section of the panel for shorter length specimens. Although only the 27.7-cm-length panel

was loaded to failure, all of the panels exhibited postbuckling strength. The 18.3-cm-long panel buckled in a local mode and the other panels buckled in a twisting mode. There is satisfactory correlation in buckle pattern, as shown in Fig. 6, between the experimental moiré fringes and the analytical curves.

Discussion of Experiment/Analysis Correlation

Results of the previous sections indicate that it is important to select the proper boundary conditions in correlating test results with analysis for short length composite panels tested with flat-end restraint conditions. Poisson's ratio for laminates composed of 0° and $\pm 45^\circ$ oriented plies is usually very high, and the resulting large biaxial stress field near the ends for flat-end tested specimens may cause them to buckle at lower strains than if the ends were free to expand laterally.

The major cause of the difference between analysis and experiment for the *J*- and blade-stiffened specimens is believed to be nonlinear buckling behavior associated with initial imperfections present in the test panels. For both the *J*- and blade-stiffened specimens, deviations on the order of 1 mm in 76 cm in the variation from straightness of the plate segments which compose the specimen cross section were observed. The experimental buckling strains were determined using the strain reversal technique. This technique is commonly used and gives a good definition for panels that exhibit bifurcation-type buckling behavior. Such results usually correlate well with a linear elastic thin-plate (bifurcation) theory. Load shortening curves for the specimens behaved nonlinearly at or near the onset of strain reversal. Large lateral displacements on the order of 25% of the local plate segment thickness were recorded for the three *J*-stiffened specimens and for the 76-cm-long blade-stiffened specimen corresponding to the strain reversal critical strain.

The test results suggest that the *J*-stiffened specimens (which differed by 20% to 25% from the analytical results) are more sensitive to initial imperfections than the blade-stiffened specimens (which differed at most by 16%). It is believed the very thin web and skin elements of the *J*-stiffened specimens considered in this study make them more sensitive to manufacturing thickness variations and variations from straightness. The blade-stiffened specimen results suggest that very short specimens of this design are not affected significantly by initial imperfections. It appears that initial imperfections in open-section stiffened panels are sufficiently important that their effects on buckling should be studied in greater detail than the scope of this paper permits.

These preliminary comparisons between experiment and analysis, although not complete, indicate sufficient correlation to justify the use of elastic thin-plate theory as the buckling analysis for the preliminary design of composite panels. A design synthesis program in which elastic buckling theory is used for the formulation of buckling constraints is presented in the next section.

Minimum Weight Panel Design Procedure

A computational procedure called JPOP (J-Panel Optimization Procedure) has been developed for the design of minimum weight open-section stiffened panels loaded in axial compression. Nonlinear mathematical programming techniques reported in Ref. 8 are used in this design procedure in which the dimensions of the panel are the design variables and the constraints are buckling and strength. It is assumed that the compression panel is wide with many stiffeners and that the structural behavior can be modeled by a typical repeating element. The geometry and design variables used to represent the repeating element for the *J*-configuration are shown in Fig. 7. The cross section is composed of four characteristic elements: 1) the skin between the attached flange, 2) the attached flange, 3) the web, and 4) the outstanding flange. The *J*-configuration reduces to the blade configuration when the outstanding flange is omitted. Seven thicknesses and four width dimensions constitute the design variables for the *J*-configuration. These reduce to six thicknesses and three width

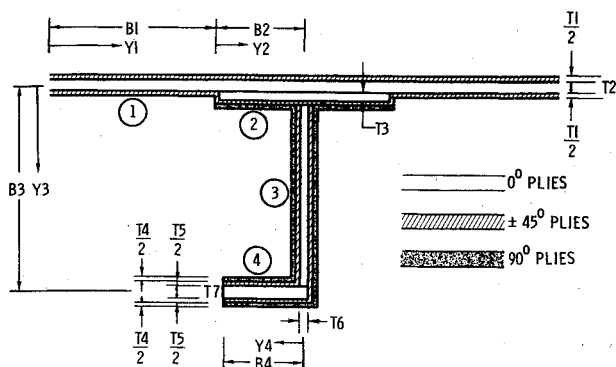


Fig. 7 JPOP configuration options and design variables.

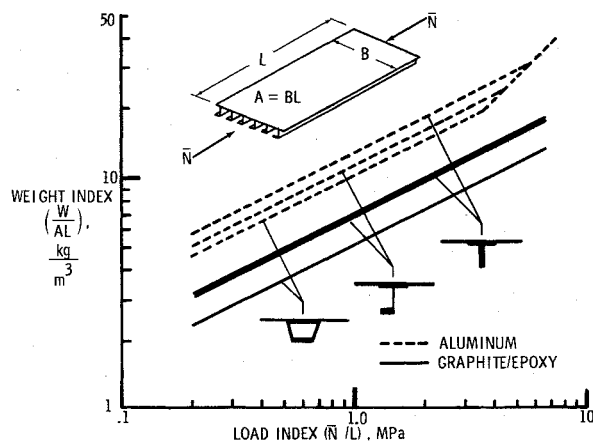


Fig. 8 Compression load structural efficiency comparison for hat-, J-, and blade configurations. Hat-configuration data taken from Ref. 2. ($\text{kg}/\text{in}^3 = 36.1 \text{ } \mu\text{lbm}/\text{in}^3$, $\text{MPa} = 145 \text{ lb}/\text{in}^2$)

dimensions for the blade. Laminae ply orientation angles of 0° , 90° , and $\pm 45^\circ$ are permitted. Orthotropic stiffnesses are assumed for all elements; thus, the anisotropic effects introduced by nonsymmetric layup patterns are ignored. The loaded ends of the panel are assumed to be simply supported. This boundary condition assumption is commonly made in the preliminary design of aircraft wing structures where the compression cover is supported by the intermediate ribs of the wing box. A discussion of the analyses used in formulating the constraints used in the JPOP program is presented in the next section.

Formulation of Design Constraints

Buckling

As discussed earlier in the paper, sophisticated theory is required to address the complex twisting mode buckling behavior of open-section stiffened compression panels. Exact theory solutions typically have execution times that are longer than is desirable for the many buckling calculations required in a design synthesis program. For this purpose, a rapid simplified buckling analysis was developed which includes all the important buckling modes characteristic of open-section compression panels but which is at least an order of magnitude faster than exact solution programs. A description of this simplified theory is presented in Appendix A, and a comparison of buckling results obtained from the simplified and exact analysis for typical J- and blade-configurations is presented in Appendix B. A buckling constraint is formulated based on this simplified theory in which the panel must not buckle at loads less than the specified design load. As discussed in Appendix A, the simplified buckling theory is capable of analyzing all of the mode shapes shown on Fig. 1 except the one labeled local/skin buckling. A separate buckling con-

straint was formulated to address this mode in which the skin is assumed to buckle as an orthotropic plate of width $2(B1 + B2)$ and to be simply supported along all its edges. This local skin buckling constraint is conservative in most cases since it does not include the effects of the additional material in the attached flange. In general, it was found that this constraint does not increase the panel design weight appreciably but may force the stiffeners to be more closely spaced than is necessary.

Transverse Shear

Two types of transverse shear can be important factors influencing the buckling load capability of compression panels. The first type, referred to as column transverse shear, is important for heavily loaded panels in which the web has low in-plane shear stiffness. Column transverse shear effects are accounted for in the JPOP design program by means of a constraint that required the load to be less than that calculated from the following expression (taken from Ref. 9)

$$\bar{P} = P_e / \left(1 + \frac{P_e}{GA} \right)$$

where GA is the inplane shear stiffness of web, and P_e is the Euler wide column buckling load.

The second type of transverse shear involves shear deformation through the thickness of the plate segment which becomes increasingly important as the ratio of the thickness to the width of the segment increases. Transverse shear of this type is not included in the JPOP synthesis code.

Strength

The material strength constraint used in JPOP limits the value of strain imposed in the direction of loading to be less than a specified value. This approach has been found satisfactory for panels loaded in compression.²



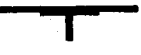



Minimum Weight Panel Design Results

The JPOP design procedure was used to determine minimum weight designs required to carry a specified load for J- and blade-stiffened configurations for both graphite/epoxy and aluminum material systems. Materials properties used in these studies are presented in Table 1. Thicknesses were assumed to be continuous variables (i.e., an integer number of plies was not required) and neither thickness nor width dimension design variables were constrained to minimum limits.

A structural efficiency curve, such as those shown in Fig. 8 was typically developed by first generating with the JPOP procedure 10 minimum weight designs in the load index (\bar{N}/L) range from 0.2 to 7 MPa. The load-carrying performance of these designs was then accurately determined using an exact analysis (BUCLASP-2)⁵ in which a typical repeating element of the cross section was analyzed. For the exact analysis model, eccentricity effects created by the attached flange were included. The simplified and exact analyses agreed within 5% for the blade-configuration, but the simplified results were 15% to 20% high for the J-configuration. These trends are consistent with the simplified and exact analysis buckling results and the corresponding panel weights were then used for plotting the structural efficiency curves for the open-section stiffened panels shown in Fig. 8. Results are also presented in Fig. 8 for a hat-stiffened configuration taken from Ref. 2.

The graphite/epoxy J- and blade-configurations have similar structural efficiencies with the J- configuration being approximately 3% more efficient than the blade (i.e., require 3% less weight to carry the same load). The graphite/epoxy J- and blade-configurations have structural efficiencies that are approximately 30% greater than the aluminum hat. The aluminum J-configuration is approximately 10% more efficient than the aluminum blade, but 11% less efficient than the aluminum hat-configuration. These results for aluminum

Table 2 Structural efficiency coefficient K for buckling critical panels

CONFIGURATION	MATERIAL	$K,^a$ $\frac{G}{Nm} (IN^{-1})$	$\frac{K}{K_{G/E \text{ HAT}}}$
	GRAPHITE/EPOXY	5.27×10^{-3} (1.58×10^{-5})	1.0
	GRAPHITE/EPOXY	6.97×10^{-3} (2.09×10^{-5})	1.32
	GRAPHITE/EPOXY	7.20×10^{-3} (2.16×10^{-5})	1.37
	ALUMINUM	10.5×10^{-3} (3.16×10^{-5})	2.0
	ALUMINUM	11.7×10^{-3} (3.52×10^{-5})	2.22
	ALUMINUM	13.0×10^{-3} (3.90×10^{-5})	2.47

$$^a K = \frac{W}{AL} \left(\frac{N}{L} \right)^{1/2}$$

are in good agreement with the lower bound for experimental data on aluminum open- and closed-section compression panel data generated by the NACA and summarized in Ref. 2.

The weight required for stability critical structures has been shown to be proportional to the square root of the panel load-carrying capability.¹⁰ This relationship may be expressed as

$$\frac{W}{AL} = K \left(\frac{N}{L} \right)^{1/2}$$

where K is the structural efficiency coefficient. The structural efficiency coefficient for each of the configurations presented in Fig. 8 is listed in Table 2. This coefficient can serve as a measure of relative merit for various configurations and material systems. In Table 2, the structural efficiency coefficient for each of the configurations has been normalized by the structural efficiency coefficient for the graphite/epoxy hat-configuration. A minimum-weight aluminum J -configuration, for example, is 2.22 times heavier than the corresponding minimum weight graphite/epoxy hat configuration designed to carry an identical compression load.

For high values of the load index, the material strength constraint becomes critical. For aluminum, with an ultimate strain of 0.0068, the strength constraint becomes critical when $N/L = 3.45$ MPa. For graphite/epoxy, with an assumed ultimate strain of 0.008, the strength constraint becomes active beyond the range of the graph. An ultimate strain lower than 0.008 could be imposed for the design of graphite/epoxy flight components when fatigue, damage-tolerance characteristics, and other factors are considered. A lower design strain would reduce the N/L value at which strength begins to govern the structural efficiency. The strength constraint effect on structural efficiency imposes a linear, limiting relationship between weight and load index that can be expressed as

$$\frac{W}{AL} = \frac{\rho}{E_{11}\epsilon} \frac{N}{L}$$

The quantities $\rho/E_{11}\epsilon$ for the materials used in this study are listed in Table 1.

Commercial Aircraft Wing Panel Designs

The wing structure of a commercial aircraft must satisfy several design requirements including strength, buckling, bending stiffness, and torsional stiffness. Bending and torsional

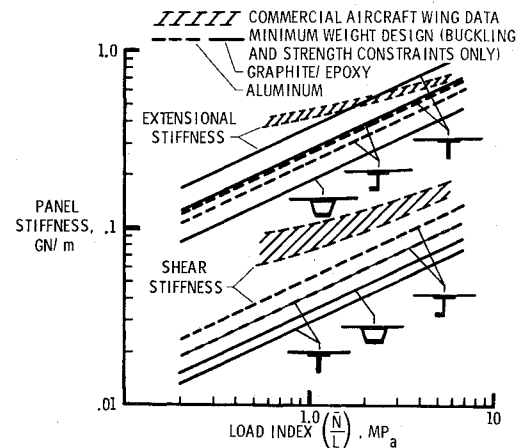


Fig. 9 Extensional and shear stiffnesses of minimum-weight panels designed to meet stability and strength constraints compared with stiffness requirements for aluminum medium-size commercial aircraft wing panels. Hat-configuration and aircraft data taken from Ref. 3. $GN/m = 5.71 \text{ Mlb/in.}$, $MPa = 145 \text{ lb/in.}^2$

stiffness requirements for medium-size commercial aircraft have been expressed as panel extensional and shear stiffness requirements³ and are shown crosshatched in Fig. 9 as a function of the compression load index. These requirements are compared in Fig. 9 with the extensional and shear stiffness properties available from minimum-weight panels designed to meet buckling and strength constraints only without extensional and shear stiffness requirements. The buckling and strength constraints only curves for extensional and shear stiffness are typical for the designs used to plot Fig. 8. For composite panels the 0° oriented material provides the primary contribution to extensional stiffness and the $\pm 45^\circ$ material in the skin and attached flange provides the primary panel shear stiffness. The stiffness curves (Fig. 9) for the graphite/epoxy designs (buckling and strength constraints only) can be shifted slightly higher or lower with little change in the panel structural efficiency by varying the percentage of 0° and $\pm 45^\circ$ oriented material in the panel cross section. For example, the shear stiffness of a blade configuration design (which plots as the lowest curve of Fig. 9) can be increased by adding $\pm 45^\circ$ material to the skin and attached flange. To maintain approximately the same panel structural efficiency, however, the percentage of 0° oriented material in the cross section must correspondingly be reduced, and the panel extensional stiffness is consequently reduced. A configuration which exhibits high structural efficiency when designed to meet buckling and strength constraints only (such as the graphite/epoxy hat, Fig. 8) has lower stiffness properties than less efficient configurations because less material is available in the cross section.

The minimum weight required for graphite/epoxy blade stiffened panels designed to meet aircraft extensional and shear stiffness requirements as well as strength and buckling is presented in Fig. 10. The minimum weight required for aluminum aircraft wing designs is shown crosshatched in Fig. 10. The graphite/epoxy blade configuration is shown to provide approximately 50% weight savings compared to the aluminum wing panel designs.

For the graphite/epoxy blade configuration to meet the aircraft shear stiffness requirements shown on Fig. 9, it is necessary to provide more $\pm 45^\circ$ oriented material in the skin and attached flange than was required to meet buckling and strength constraint requirements only. Also, a greater quantity of 0° oriented material is required in the cross section for lower ranges of the load index (0.6 to 2 MPa); however, less 0° oriented material is required in the higher load index range (2 to 5 MPa).

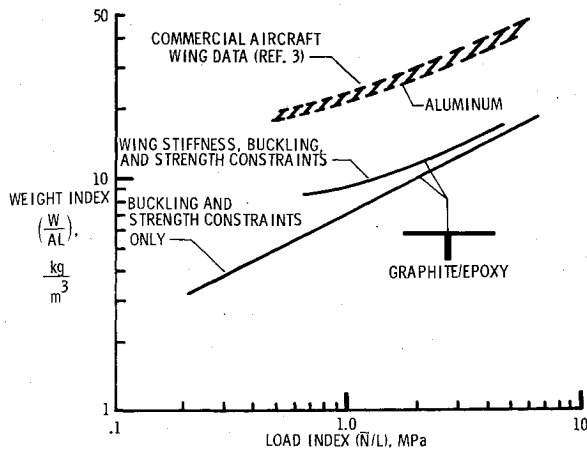


Fig. 10 Structural efficiency of graphite/epoxy blade-stiffened compression panel designed to meet medium-size commercial aircraft wing stiffness stability, and strength requirements and comparison with other data. ($\text{kg/m}^3 = 36.1 \text{ lbm/in.}^3$, $\text{MPa} = 145 \text{ lb/in.}^2$.)

For comparison, the structural efficiency curve from Fig. 8 for the graphite/epoxy blade-configuration designed to meet buckling and strength constraints only is repeated in Fig. 10. Since this curve represents designs which already meet buckling requirements, the ordinate difference between the two graphite/epoxy blade curves represents the additional mass which is required to meet the extensional and shear stiffness requirements. When large differences in mass exist between these two curves, the stiffness critical design may not necessarily be buckling critical at the design load. This provides the designer with the flexibility to distribute the additional material in the cross section to increase the actual buckling load above the required design load.

Concluding Remarks

Exploratory experiments were conducted on graphite/epoxy open-section stiffened panels to study their buckling behavior. Local, twisting, and column buckling modes with interaction between these modes were found to characterize the buckling behavior of open-section *J*- and blade-stiffened compression panels. It was found that the buckling behavior of short-length panels is influenced by the flat-end boundary conditions used in testing. To determine analytically this buckling behavior, it is necessary to account for the prebuckling stress field associated with clamped edges including zero inplane displacements. Correlation of experimental with exact analytical (bifurcation) results which included these inplane displacement restraints indicated that the buckling strains of *J*-stiffened specimens were 75% to 80% of the analytical values and blade-stiffened panels were 84% to 97% of the analytical values. A nonlinear response was exhibited by several of the specimens in which large lateral displacement on the order of one-quarter of the thickness of the panel plate segments were observed corresponding to the experimentally defined strain reversal buckling strain.

Sufficient correlation of experimental and analytical buckling modes and strains was obtained to justify the use of thin-plate buckling theory for the preliminary design of open-section composite compression panels. A rapid, simplified buckling analysis based on thin-plate theory was formulated and used for the purpose of generating design constraints in a minimum weight design synthesis computer code for open-section stiffened panels. This design code (which includes strength as well as buckling constraints) was used to determine trends for the relative structural efficiency of *J*- and blade-stiffened compression panels made of both graphite/epoxy and aluminum. These results show that open-section stiffened graphite/epoxy panels can be designed to carry a specified

compression load with 30% less weight than is required by the most efficient aluminum configuration. A study was also conducted on the structural efficiency of a graphite/epoxy blade-stiffened panel design which may have manufacturing advantages due to its geometric simplicity. When the extensional and shear stiffness requirements of commercial aircraft are taken into account the graphite/epoxy blade-stiffened panel shows a 50% weight savings when compared to existing aluminum wing panels.

Appendix A: Simplified Buckling Analysis

A simplified buckling analysis is developed for open-section *J*- and blade-stiffened wide panels loaded in axial compression. It is assumed in the development of this analysis that the buckling of a wide multistiffened panel may be analyzed by studying the buckling response of a single repeating element of the panel cross section. The repeating element model for the *J*-configuration is composed of six basic plate segments and is similar in cross section to that shown in Fig. 7 except that the skin and attached flange have a common center line. The skin and attached flange of the repeating element may deflect in either a symmetric or antisymmetric manner. However, the displacement functions assumed herein restrict the deformations to an antisymmetric mode. The skin and attached flange on each side of the web are assumed to behave similarly even though the outstanding flange segment makes the single repeating *J*-element asymmetric. The error associated with the previous assumption was studied using the exact analysis of Ref. 5. In this study, a panel composed of several (up to six) repeating *J*-elements was found to give solutions that are within 5% of that found by analyzing a single repeating element.

The virtual work done by each plate segment of the cross section during buckling may be expressed as

$$\delta\pi = \int_0^B \int_0^L [N_x \delta\epsilon_x + N_y \delta\epsilon_y + N_{xy} \delta\gamma_{xy} + M_x \delta\kappa_x + M_y \delta\kappa_y + M_{xy} \delta\kappa_{xy} - \epsilon_{x_{av}} \left(A_{11} - \frac{A_{12}^2}{A_{22}} \right) (w_{,x} \delta w_{,x} + v_{,x} \delta v_{,x})] dx dy$$

where the N 's and M 's are the stress resultants and moments, the ϵ 's, γ_{xy} , and κ 's are the strains and curvatures, and w and v are deformations that occur during buckling. The axial length of the panel is L and the width of each segment is B_i . Each segment may have a different load applied to it, but the prebuckling axial strain $\epsilon_{x_{av}}$ is the same. Since the repeating element is assumed free to expand prior to buckling, the proper coefficient of $\epsilon_{x_{av}}$ in terms of the orthotropic extensional stiffnesses A_{ij} is present. The virtual work expression includes the work of extension and bending during buckling. It also includes the work of the applied strain during buckling from terms that correspond to those in the nonlinear strain expression

$$\epsilon_{x_{NL}} = u_{,x} + \frac{1}{2} (w_{,x}^2 + v_{,x}^2)$$

which are required^{5,6} in order to account for inplane motion of the web and outstanding flange. For the strains and curvatures that appear in this virtual work expression and in the stress-strain and moment-curvature relations used, only the linear expressions

$$\begin{aligned} \epsilon_x &= u_{,x} & \kappa_x &= -w_{,xx} \\ \epsilon_y &= v_{,y} & \kappa_y &= -w_{,yy} \\ \gamma_{xy} &= u_{,y} + v_{,x} & \kappa_{xy} &= -2w_{,xy} \end{aligned}$$

and

$$\begin{aligned} N_x &= A_{11}\epsilon_x + A_{12}\epsilon_y & M_x &= D_{11}\kappa_x + D_{12}\kappa_y \\ N_y &= A_{22}\epsilon_y + A_{12}\epsilon_x & M_y &= D_{22}\kappa_y + D_{12}\kappa_x \\ N_{xy} &= A_{66}\gamma_{xy} & M_{xy} &= D_{66}\kappa_{xy} \end{aligned}$$

are necessary.

The total virtual work is equal to the sum of the virtual work for each of the six segments. By substituting the above expression for the forces and moments and the strains and curvatures, the virtual work equation can be expressed in terms of the u , v , w for each segment. The method of virtual work can then be used to solve the characteristic value problem for the lowest $\epsilon_{x_{av}}$ by considering general u , v , w (or approximately by considering particular u , v , w) that satisfy boundary and continuity conditions. The u , v , w displacements that have been chosen for the simple buckling analysis presented here are listed below for each of the plate segments.

Segment

	u	v
1	$U_1 \cos \frac{m\pi x}{L}$	0
2	$U_2 \cos \frac{m\pi x}{L}$	0
3	$(U_{30} + U_3 y_3) \cos \frac{m\pi x}{L}$	$V_3 \sin \frac{m\pi x}{L}$
4	$(U_{40} + U_4 y_4) \cos \frac{m\pi x}{L}$	$V_4 \sin \frac{m\pi x}{L}$

Segment

	w
1	$(W_{10} + W_1 \cos \frac{\pi y_1}{2B_1}) \sin \frac{m\pi x}{L}$
2	$(W_{20} + W_2 y_2) \sin \frac{m\pi x}{L}$
3	$[W_3 \sin \frac{\lambda y_3}{B_3} + W_{30}(1 - \cos \frac{\gamma y_3}{B_3})] \sin \frac{m\pi x}{L}$
4	$(W_{40} + W_4 y_4) \sin \frac{m\pi x}{L}$

where the U 's, V 's, and W 's are constants.

These displacements were chosen so that they would satisfy simple support boundary conditions at $x=0, L$, and have zero slope at $y_1=0$ and the corresponding point on the other side of the repeating element. The simplest possible displacement functions were chosen in the Y direction that would give reasonable results for buckling in the local, stiffener twisting, and column modes. By assuming the expressions given for w in segments 1 and 2, accuracy in the local/skin only mode has been sacrificed for simplicity. Except for the w deflection of the skin and web, the displacements are zero, constant, or linear in the Y direction. The skin deflection expression has a trigonometric function in the Y direction to allow local buckling and twisting. The web deflection expression has two trigonometric functions in the Y direction plus arbitrary parameters λ and γ to allow for rolling as well as local buckling and twisting.

The assumed displacement in the skin and the attached flange lead to zero inplane shearing strain, γ_{xy} . An additional assumption is made that the web and outstanding flange also have zero inplane shearing strain. Ten geometric continuity

conditions must be satisfied between the various elements in addition to the two already satisfied. Satisfaction of the continuity conditions and the shear strain assumption can be used to reduce the number of unknown U 's, V 's, and W 's from 16 to 4.

Thus, for a given design, the method of virtual work gives results in the form of four equations in four unknowns to determine $\epsilon_{x_{av}}$ as a function of λ and γ . An exploratory study indicated that for a given design it is sufficient to set $\epsilon_{x_{av}}$ equal to the lowest $\epsilon_{x_{av}}$ solution to the equations from the virtual work with λ equal to one of the following trial values $0.1\pi, 0.3\pi, 0.5\pi, 0.7\pi$ and $\gamma = \lambda + 0.5\pi$. Local buckling results are obtained with the lowest value of $\lambda(0.1\pi)$. Twisting results are obtained with intermediate values of $\lambda(0.3\pi$ and $0.5\pi)$, and column buckling results are obtained with the highest value of $\lambda(0.7\pi)$.

Appendix B: Comparison of Simplified and Exact Buckling Solutions

Buckling strains calculated using the simplified analysis (Appendix A) and the exact analysis^{5,6} for minimum-weight J - and blade-configuration designs are presented in Figs. 11 and 12 as a function of the buckle wavelength. Cross-section details of these designs are also presented on those figures.

J-Configuration

Results for the J -stiffened design plotted in Fig. 11 show the simplified analysis results follow the same trend as the exact analysis results. This agreement demonstrates the ability of the simplified analysis to account for the important buckle modes characteristic of open-section panels. The column and minimum local buckling mode solutions are in good agreement with the exact theory; however, the twisting buckling mode strain for the simplified analysis is approximately 20% higher than the exact analysis. In this example and in other results, the simplified analysis was found to determine the buckling strain of the important modes for the J -configuration to within 20%.

Blade Configuration

Results for the blade-stiffened design plotted in Fig. 12 show that results from the simplified analysis follow the same trend as results from the exact analysis. Instead of the two minima that appear in the curve for the J -configuration, only one minimum appears for the blade-configuration due to the absence of the outstanding flange. Close agreement (within approximately 3%) between the simplified and exact analyses is shown in Fig. 12 for the column and twisting buckling modes. For local mode wavelengths (between 4 and 10 cm) the skin buckles in a symmetric mode (local/skin only) permitting the stiffener to remain undeformed. The 10% difference between the simplified and exact theory results for this local mode occurs because the displacement functions assumed for

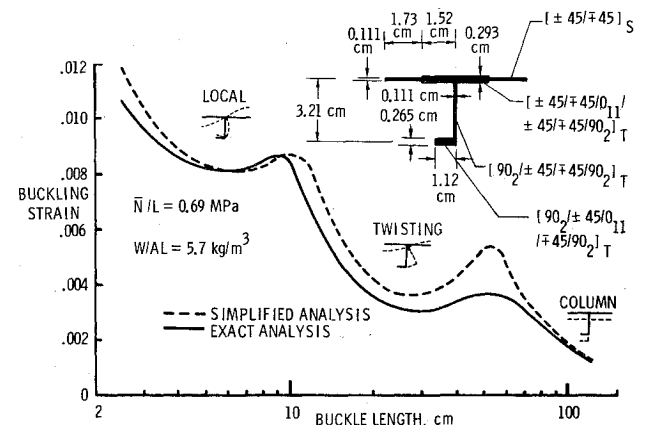


Fig. 11 Comparison of exact and simplified analyses for buckling strain of J -configuration as a function of the panel buckle length.

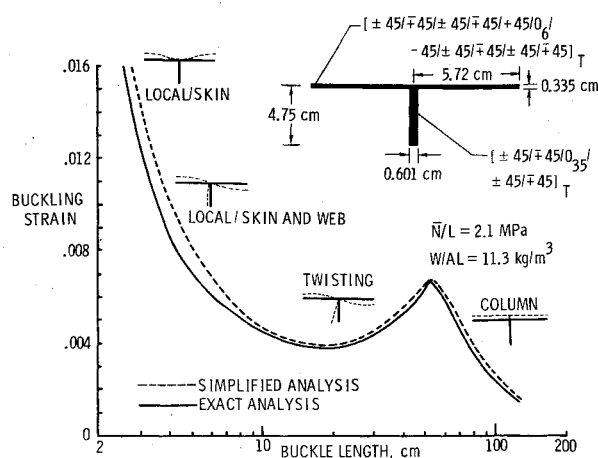


Fig. 12 Comparison of exact and simplified analyses for buckling strain of blade-configuration as a function of the panel buckle length.

the simplified theory were not general enough to represent adequately this symmetric skin buckling mode.

References

¹Agarwal, B. L. and Davis, R. C., "Minimum-Weight Designs for Hat-Stiffened Composite Panels Under Uniaxial Compression," NASA TN D-7779, 1974.

²Williams, J. G. and Mikulas, M. M., Jr., "Analytical and Experimental Study of Structurally Efficient Composite Hat-Stiffened Panels Loaded in Axial Compression," AIAA Paper 75-754, Denver, Colo., 1975, (also available as NASA TM X-72813).

³Mikulas, M. M., Jr., Bush, H. G., and Rhodes, M. D., "Current Langley Research Center Studies on Buckling and Low-Velocity Impact of Composite Panels," Presented at the *Third Conference on Fibrous Composites in Flight Vehicle Design*, Williamsburg, Va., Nov. 4-6, 1975.

⁴Almroth, B. O., Brogan, F. A., and Marlow, M. B., "Collapse Analysis for Shells of General Shape. Volume I, Analysis," Air Force Flight Dynamics Lab., Wright-Patterson Air Force Base, Ohio, AFF-DL-TR-71-8, Aug. 1972.

⁵Viswanathan, A. V. and Tamekuni, M., "Elastic Buckling Analysis for Composite Stiffened Panels and Other Structures Subjected to Biaxial Inplane Loads," NASA CR-2216, March 1973.

⁶Wittrick, W. H. and Williams, F. W., "Buckling and Vibration of Anisotropic or Isotropic Plate Assemblies Under Combined Loadings," *International Journal of Mechanical Science*, Vol. 16, 1974.

⁷Dykes, B. C., "Analysis of Displacements in Large Plates by the Grid-Shadow Moire Technique," *Fourth International Conference on Experimental Stress Analysis*, Cambridge, England, 1970.

⁸Jones, R. T. and Hague, D. W., "Application of Multivariable Search Techniques to Structural Design Optimization," NASA CR-2038, 1972.

⁹Timoshenko, S. P. and Gere, J. M., *Theory of Elastic Stability*, McGraw-Hill, N. Y., 1961.

¹⁰Gerard, G., *Minimum Weight Analysis of Compression Structures*, New York University Press, N. Y., 1956.

From the AIAA Progress in Astronautics and Aeronautics Series . . .

INSTRUMENTATION FOR AIRBREATHING PROPULSION—v. 34

Edited by Allen Fuhs, Naval Postgraduate School, and Marshall Kingery, Arnold Engineering Development Center

This volume presents thirty-nine studies in advanced instrumentation for turbojet engines, covering measurement and monitoring of internal inlet flow, compressor internal aerodynamics, turbojet, ramjet, and composite combustors, turbines, propulsion controls, and engine condition monitoring. Includes applications of techniques of holography, laser velocimetry, Raman scattering, fluorescence, and ultrasonics, in addition to refinements of existing techniques.

Both inflight and research instrumentation requirements are considered in evaluating what to measure and how to measure it. Critical new parameters for engine controls must be measured with improved instrumentation. Inlet flow monitoring covers transducers, test requirements, dynamic distortion, and advanced instrumentation applications. Compressor studies examine both basic phenomena and dynamic flow, with special monitoring parameters.

Combustor applications review the state-of-the-art, proposing flowfield diagnosis and holography to monitor jets, nozzles, droplets, sprays, and particle combustion. Turbine monitoring, propulsion control sensing and pyrometry, and total engine condition monitoring, with cost factors, conclude the coverage.

547 pp. 6 x 9, illus. \$14.00 Mem. \$20.00 List

TO ORDER WRITE: Publications Dept., AIAA, 1290 Avenue of the Americas, New York, N. Y. 10019